Materials Science-Poland, 30(1), 2012, pp. 1-9
http://www.materialsscience.pwr.wroc.pl/
DOI: 10.2478/s13536-012-0002-7

VERSITA

Study of magnetic inhomogeneity in β-$Cu_3Fe_4V_6O_{24}$*

N. GUSKOS[1,2†], G. ZOLNIERKIEWICZ[2], J. TYPEK[2], R. SZYMCZAK[3], A. BLONSKA-TABERO[4]

[1]Solid State Physics, Department of Physics, University of Athens, Panepistimiopolis, 15 784 Zografos, Athens, Greece

[2]Institute of Physics, West Pomeranian University of Technology, Al. Piastow 48, 70-311 Szczecin, Poland

[3]Institute of Physics, Polish Academy of Sciences, Al. Lotnikow 36/42, 02-688 Warsaw, Poland

[4]Department of Inorganic and Analytical Chemistry, West Pomeranian University of Technology, Al. Piastow 42, 70-065 Szczecin, Poland

The temperature dependence of dc magnetization and electron paramagnetic resonance (EPR) spectra of the β-$Cu_3Fe_4V_6O_{24}$ multicomponent vanadate were investigated. Dc magnetic measurements showed the presence of strong antiferromagnetic interactions (Curie-Weiss temperature, $\Theta \sim 80$ K) at high temperatures, while zero-field-cooled (ZFC) magnetization revealed a cusp-like maximum in low fields at $T_{f1} = 4.4$ K, which coincides with the splitting of the ZFC and FC curves. Another maximum was registered at $T_{f2} = 3.0$ K. These two temperatures (T_{f1} and T_{f2}) could be regarded as freezing temperatures in the spin glass state of two magnetic sublattices of Fe1 and Fe2 ions. The EPR spectrum of β-$Cu_3Fe_4V_6O_{24}$ is dominated by a nearly symmetrical, very intense and broad resonance line centered at $g_{\text{eff}} \sim 2.0$ that could be attributed to iron ions. Below 10 K, an additional EPR spectrum with $g_1 = 2.018(1)$ and $g_2 = 2.175(1)$ appears, as well as a very weak line at $g_{\text{eff}} = 1.99(1)$. The former spectrum is probably is due to divalent copper ions, and the latter line due to vanadium V^{4+} complexes. The temperature dependence of EPR parameters (g-factor, linewidth, integrated intensity) was determined in the range of 3 – 300 K. Two low-temperature maxima in the temperature dependence of the integrated intensity (at 40 and 6 K) were fitted with a function suitable for pairs of exchange-coupled Fe^{3+} ions. A comparison of dc magnetic susceptibility and EPR integrated intensity indicates the presence of spin clusters, which play an important role in determining the low-temperature magnetic response of β-$Cu_3Fe_4V_6O_{24}$.

Keywords: *EPR vanadates*

1. Introduction

The $M_2FeV_3O_{11}$ and $M_3Fe_4V_6O_{24}$ (M(II) = Mg(II), Zn(II), Mn(II), Cu(II), Ni(II) and Co(II)) multicomponent vanadates are intensively investigated because of their interesting physical properties, in particular the magnetic ones [1–6]. These systems have a very complicated magnetic structure with the presence of different sublattices of magnetic ions and disorder in the cation positions [7–11]. The Curie-Weiss temperature of $M_2FeV_3O_{11}$ compounds is almost twice as low as that of $M_3Fe_4V_6O_{24}$ and the disorder processes in these compounds are more intense [3, 4, 7, 8] despite the fact that the number of non-equivalent sublattices with magnetic ions is smaller [5, 6, 9, 10]. Additionally, $M_3Fe_4V_6O_{24}$ compounds, like other vanadate systems, are spin-frustrated systems [12–14]. High-frequency electron paramagnetic resonance (EPR) measurements showed that in $Mn_3Fe_4V_6O_{24}$ antiferromagnetic (AFM) interactions coexist with ferromagnetic (FM) ones [6]. Magnetic measurements showed that in the $M_3Fe_4V_6O_{24}$ system, there occurs a strong AFM interaction at high temperatures, which depends on the type of cation. Moreover, EPR measurements showed that competition between strong magnetic interactions prevents the formation of magnetic order at high temperatures [15]. Site substitution of magnetic

*This paper was presented at the Conference Functional and Nanostructured Materials, FNMA 11, 6-9 September 2011, Szczecin, Poland

†E-mail: ngouskos@phys.uoa.gr

ions in place of the diamagnetic ions can change significantly even the crystalline structure [16].

There are two vanadates containing iron and copper, which are chemically similar, but differ in their three-dimensional structure: orthorhombic lyonsite $Cu_3Fe_4V_6O_{24}$ and triclinic β-$Cu_3Fe_4V_6O_{24}$ [1]. The latter is the subject of this study. The crystal structure of β-$Cu_3Fe_4V_6O_{24}$ is closely related to howardevansite and contains edge-sharing octahedral dimers of iron, connected by VO_4 tetrahedra, as well as two types of copper polyhedra, viz. square planes and trigonal bipyramids (see Fig. 1). There are two octahedral iron sites: Fe1 and Fe2 in the crystal structure. Both Fe octahedra form edge-sharing dimeric clusters. Cationic disorder between octahedral iron and fivefold coordinated copper sites have been detected by Mössbauer spectroscopy [1]. Susceptibility measurements in the 20 – 250 K range have shown the presence of strong AFM interactions and possible AFM phase transition at $T_N \approx 15$ K [1]. Considerable variation of the ordering temperature was detected by analysing hyperfine fields observed in the Mössbauer spectra of β-$Cu_3Fe_4V_6O_{24}$. This may be due to the presence of isolated clusters and cationic disorder in the metallic sublattice [1]. Despite these observations, the low-temperature magnetic state of β-$Cu_3Fe_4V_6O_{24}$ is still not fully understood.

EPR measurements of β-$Cu_3Fe_4V_6O_{24}$ have been reported in two papers [15, 17]. In Ref. [17], only the room-temperature spectrum was analysed. The EPR parameters (linewidth, g-factor, integrated intensity) were calculated and compared with those obtained from similar spectra of $M_3Fe_4V_6O_{24}$ (M = Mg, Zn, Mn, Co) compounds. In Ref. [14], EPR spectra of β-$Cu_3Fe_4V_6O_{24}$ were registered in 90 – 290 K range. The temperature gradient of the resonance field, $\Delta H_r/\Delta T$, was investigated and correlated with the distance between iron ions in the dimer. A study of this relationship in other $M_3Fe_4V_6O_{24}$ compounds suggests that the EPR spectrum is attributable to Fe1-Fe1 dimers and not Fe2-Fe2 dimers.

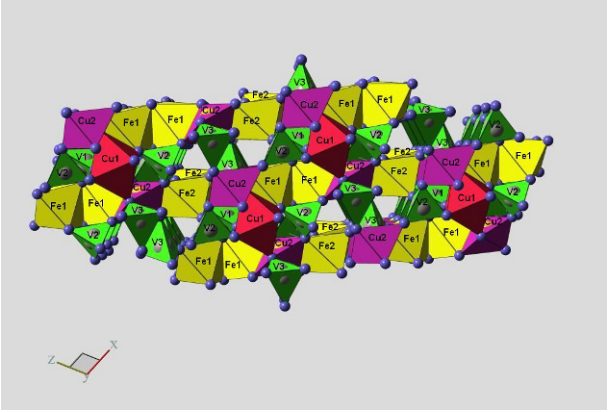

Fig. 1. The structure of β-$Cu_3Fe_4V_6O_{24}$, viewed along the [010] direction. The following coordination polyhedra of the cations are indicated: tetrahedra for V^{5+}, octahedra for Fe^{3+}, trigonal bipyramids for Cu^{2+}.

The aim of this work is to investigate the dc magnetization and the dependence of EPR spectra on temperature for β-$Cu_3Fe_4V_6O_{24}$, especially in the low temperature range. In this compound, the effects of competing magnetic interactions and frustration effects are expected to be revealed at temperatures $T < 50$ K. The presence of spin clusters is also probable. As the EPR technique seems to be particularly suitable to study these phenomena, we expect to gain a comprehensive understanding of magnetic properties of β-$Cu_3Fe_4V_6O_{24}$.

2. Experimental

A polycrystalline sample of the β-$Cu_3Fe_4V_6O_{24}$ multicomponent vanadate was prepared by solid-state reaction between 80 mol.% $FeVO_4$ and 20 mol.% $Cu_3(VO_4)_2$ [18]. The crystal structure of $Cu_3Fe_4V_6O_{24}$ was investigated by X-ray diffraction (XRD) and the following lattice parameters were determined: a = 6.600(3) Å, b = 8.048(4) Å, c = 9.759(5) Å, $\alpha = 106.08(3)^\circ$, β = 103.72(3)°, and γ = 102.28(2)° [1]. This corresponds to a unit cell volume of V = 461.8 Å^3 which is the smallest among the $M_3Fe_4V_6O_{24}$ compounds (M(II) = Zn(II), Mn(II), Cu(II) and Mn(II)).

Table 1. Values of the Curie-Weiss temperature (in K) obtained from the temperature dependence of the inverse magnetic susceptibility for four compounds in the $M_3Fe_4V_6O_{24}$ system.

Magnetic field [Oe]	β-$Cu_3Fe_4V_6O_{24}$	$Mg_3Fe_4V_6O_{24}$	$Mn_3Fe_4V_6O_{24}$	$Zn_3Fe_4V_6O_{24}$
50	−82.0(5)	–	–	−101(1)
100	−81.2(5)	−115(1)	−159(1)	–
6000	−77.6(5)	–	-160(1)	−100(1)
50000	−76.8(6)	−113(1)	−152(2)	

Dc susceptibility measurements were carried out using an MPMS-5 SQUID magnetometer in the temperature range of 2 – 300 K and magnetic fields up to 50 kOe in the zero-field-cooled (ZFC) and field-cooled (FC) modes.

EPR spectra were recorded using a standard X-band spectrometer, Bruker E 500 ($\nu = 9.45$ GHz) with a magnetic field modulation of 100 kHz. The magnetic field was scaled with a NMR magnetometer. The measurements were performed in the temperature range of 3 – 290 K using an Oxford flow cryostat and a standard hot air flow system.

3. Experimental results and discussion

3.1. Dc magnetic measurements

Fig. 2 shows the temperature dependence of the inverse magnetic susceptibility (χ^{-1}), obtained from dc magnetization measurements $M_{ZFC}(T)$ for different values of the applied magnetic field. The insets a and b in Fig. 2 show this dependence in the low temperature range. A Curie-Weiss type of behavior prevails in the high temperature range. For $T > 70$ K, the Curie-Weiss fit of χ^{-1}(T) to the experimental data allowed us to obtain the value of the Curie-Weiss temperature and the effective magnetic moment. The Curie-Weiss temperatures of the isostructural $M_3Fe_4V_6O_{24}$ compounds are presented in Table 1. For the β-$Cu_3Fe_4V_6O_{24}$ compound with divalent copper ion ($3d^9$, S = 1/2), the Curie-Weiss temperature is negative and its absolute value is the smallest among the homogeneous $M_3Fe_4V_6O_{24}$ compounds (Table 1). The value of the Curie-Weiss temperature suggests the presence of AFM interactions at high temperatures, however, replacing the diamagnetic cation (Mg^{2+}) with a magnetic copper ion significantly reduces the Curie-Weiss temperature. Additionally, a reduction of the Curie-Weiss temperature with an increase in the applied magnetic field is observed. The Curie-Weiss fit to $\chi^{-1}(T)$ data for β-$Cu_3Fe_4V_6O_{24}$ yields an effective magnetic moment of 11.07 μ_B per formula unit comprising four Fe and three Cu ions. Note that the calculated $S_{\text{eff}} \sim 5$ is significantly smaller than the spin-only value S_{eff} = 23/2 for high-spin Fe^{3+} ions ($3d^5$, ground state $^6S_{5/2}$), assuming that the Cu^{2+} ions are in the S = 1/2 state. On the other hand, the obtained value of the effective magnetic moment is smaller than that observed for $Mn_3Fe_4V_6O_{24}$ (∼13 μ_B) [6]. This is to be expected, as copper ions possess a weaker magnetic moment than manganese ions. Antiferromagnetic coupling of magnetic ions seems to play an important role in the $Cu_3Fe_4V_6O_{24}$ compound.

The paramagnetic-like downturn of $\chi^{-1}(T)$ curve is observed at lower temperatures, a behavior which is frequently registered in frustrated antiferromagnets. At $T < 5$ K, the dc susceptibility exhibits a weak maximum at low fields with a significant field dependence (Fig. 3). To examine this behavior, the low-T dependence of the ZFC and FC magnetization was measured at different magnetic fields, as shown in Fig. 3. The ZFC magnetization reveals a distinct cusp-like maximum in low fields at T_{f1} = 4.4 K, which coincides with the splitting of the ZFC and FC curves, while another maximum is registered at T_{f2} = 3.0 K. At higher magnetic fields, the maximum at T_{f1} becomes gradually smeared out, signaling the presence of a spin-freezing

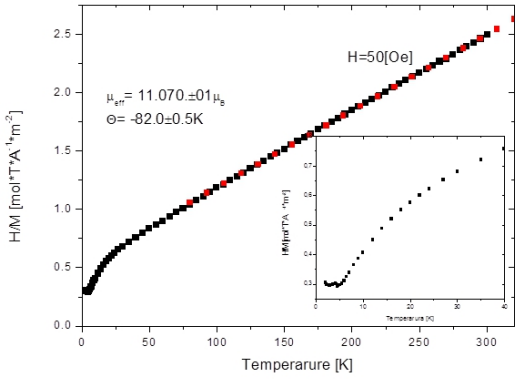

(a)

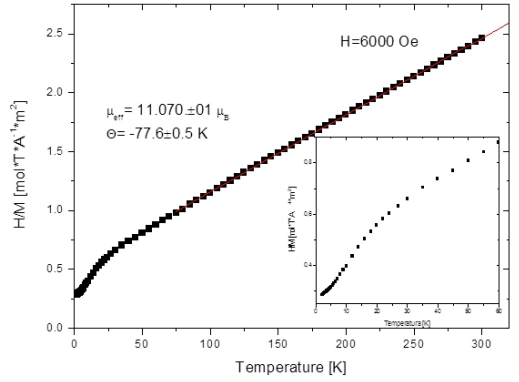

(b)

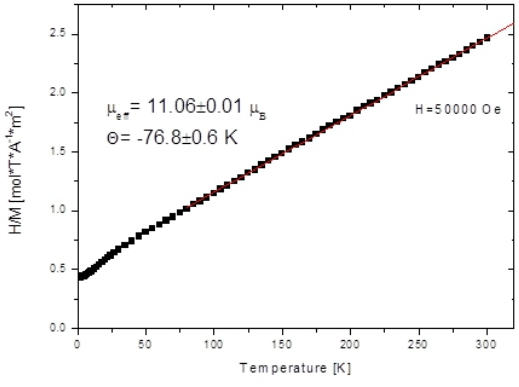

(c)

Fig. 2. Temperature dependence of the inverse magnetic susceptibility, χ^{-1}, for the β-$Cu_3Fe_4V_6O_{24}$ compound: a) at $H = 50$ Oe, b) at $H = 6$ kOe, and c) at $H = 50$ kOe. The insets in panels a and b show this dependence in the low temperature range. The solid lines show the Curie-Weiss fit at high temperatures.

transition. These two temperatures (T_{f1} and T_{f2}) could be regarded as freezing temperatures into the spin-glass state of two magnetic sublattices of Fe1 and Fe2 ions. Fig. 4 shows the plots of the temperature derivative $d(M_{ZFC}/H)/dT$ as a function of temperature for various magnetic fields. The freezing temperature T_{f1} can be clearly identified from the center of the resonance-like curve at T_{f1} = 4.40 K, where all the plots for different fields intersect. This value is significantly smaller than the corresponding temperature (8.5 K) for $Mg_3Fe_4V_6O_{24}$. A comparison of the Curie-Weiss temperature, which determines the mean-field energy scale for the AFM coupling of Fe^{3+} spins and the freezing temperatures, indicates significant spin frustration.

3.2. EPR measurements

Fig. 5(a), presents the EPR spectra at X-band for β-$Cu_3Fe_4V_6O_{24}$ taken at different temperatures. The high-temperature region is dominated by a nearly symmetrical, very intense and broad resonance line centered at $g_{\text{eff}} \sim 2.0$ that could be attributed to iron ions. Below 10 K, an additional EPR spectrum with $g_1 = 2.018(1)$ and $g_2 = 2.175(1)$ appears, as well as a very weak line at $g_{\text{eff}} = 1.99(1)$. The former spectrum is probably due to divalent copper ions and the latter line due to vanadium V(IV) complexes [19, 20]. The shape of the most intense EPR resonance lines could be satisfactorily fitted by a Lorentzian function (Fig. 5(b), and 5(c)), taking into account the contribution from the negative magnetic fields. This is a consequence of the linearly polarized rf field which becomes important when the linewidth becomes comparable to the resonance field.

Fig. 6 presents the temperature dependence of two important EPR parameters: the g-factor, and the peak-to-peak linewidth ΔH_{pp} for the main, broad line. Fig. 6(a) presents the temperature dependence of the resonance field H_r. The temperature gradient of this field ($\Delta H_r/\Delta T$) is approximately constant in three temperature regions: $\Delta H_r/\Delta T$ (290 – 85 K) = −0.08 Oe/K; $\Delta H_r/\Delta T$ (60 – 28 K) = −2.13 Oe/K; and $\Delta H_r/\Delta T$ (28 – 11 K) = 22.94(1) Oe/K. It can be observed

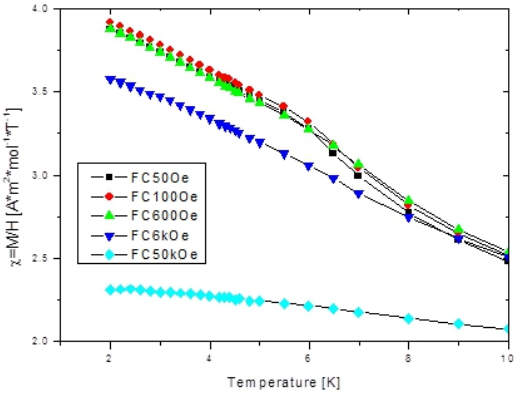

(a)

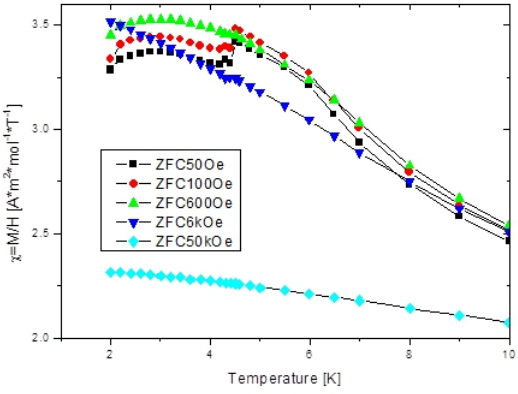

(b)

Fig. 3. Low-temperature dependence of the magnetic susceptibility, χ, for β-$Cu_3Fe_4V_6O_{24}$ in a) FC, and b) ZFC modes.

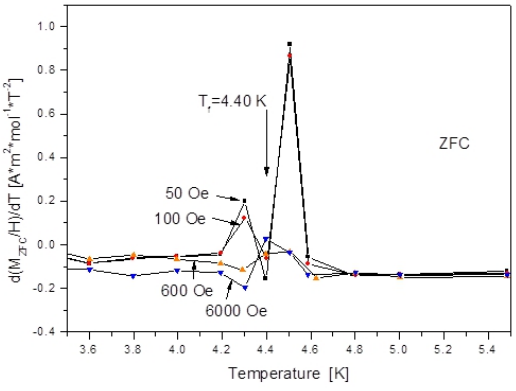

Fig. 4. Plots of the temperature derivative $d(M_{ZFC}/H)/dT$ vs. T at low temperatures for different applied fields. The arrow indicates the freezing temperature T_{f1}.

from these values that the gradient changes appreciably at certain temperatures. This change is related to reorientation processes in the spin system and it affects the spin resonance condition $h\nu = g\mu_B(H_o \pm H_{int})$, where h is the Planck constant, ν is the resonance frequency, μ_B is the Bohr magneton, H_o is the external magnetic field and H_{int} is the internal magnetic field created by the spin system. The temperature intervals of linewidth change are closely related to temperature intervals where the temperature gradient of the resonance field is constant (Fig. 6(c)). To reveal different temperature ranges corresponding to relaxation processes, a log-log plot of the linewidth ΔH_{pp} vs. the resonance field H_r was employed (see Fig. 7). In such a plot, any detected change in the slope is indicative of a change in the relaxation type in the investigated sample. This kind of plot is often used when dealing with superparamagnetic particles with a statistical distribution of shapes and sizes [21]. In the case of our sample, the change in the $\log(\Delta H_{pp})/\log(H_r)$ slope might indicate a change of the relaxation mechanism. Closer scrutiny of Fig. 7 reveals the existence of three temperature ranges. The limiting temperatures are 75 K and 29 K, separating the intermediate temperature range from the high and low ranges.

In Fig. 8, the temperature dependence of another important parameter, i.e. the EPR integrated intensity I_{int}, is presented. The EPR integrated intensity, calculated as the area under the absorption curve of the main, broad line, is proportional to the dynamic magnetic susceptibility of the spin system at microwave frequency. As can be seen in Fig. 8(a), I_{int} reaches a maximum at c.a. 40 K on cooling from RT, but below 15 K it starts to increase once again with further cooling and reaches another maximum at

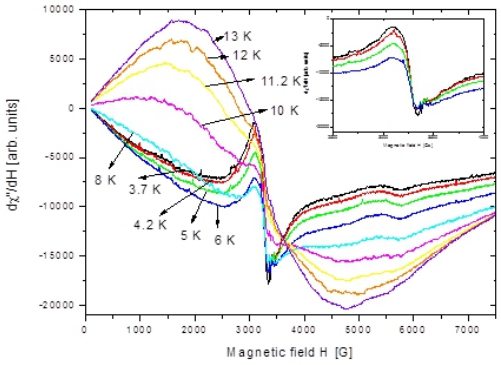

(a)

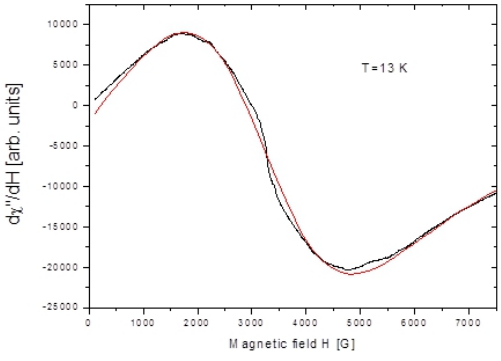

(b)

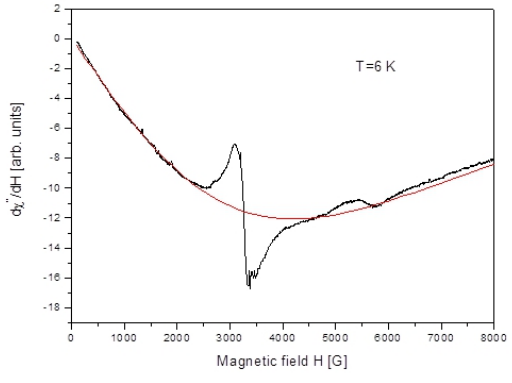

(c)

Fig. 5. EPR spectra of β-$Cu_3Fe_4V_6O_{24}$: a) at different temperatures in the low temperature range; b) the shape of the most intense EPR resonance line fitted by a Lorentzian function at T = 13 K; c) the shape of the most intense EPR resonance line fitted by a Lorentzian function at T = 6 K.

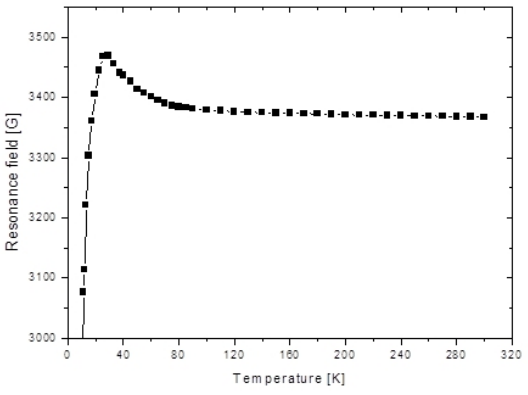

(a)

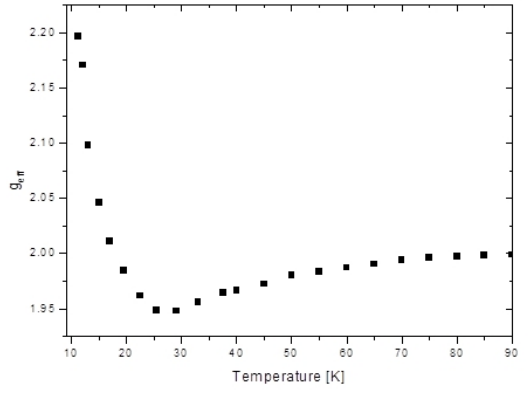

(b)

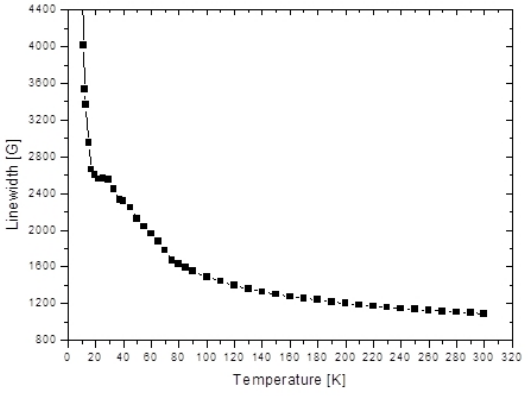

(c)

Fig. 6. Temperature dependence of: a) resonance field H_r; b) the g-factor, and c) linewidth ΔH_{pp} of the main resonance line.

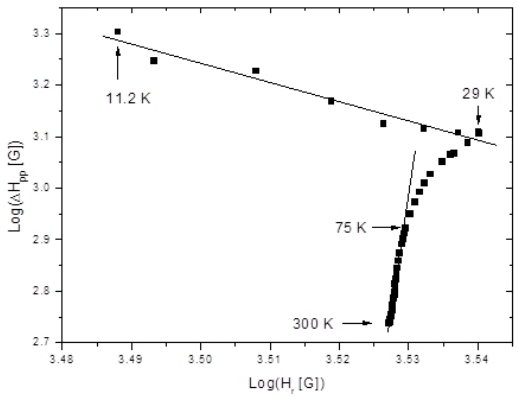

Fig. 7. Log-log plot of the linewidth ΔH_{pp} vs. the resonance field H_r.

6 K. An attempt was made to fit these two local maxima with the function obtained for Fe^{3+}–Fe^{3+} pairs. In the strong isotropic exchange limit, the discrete energy spectrum of a Fe^{3+}–Fe^{3+} pair consists of six states of total spin S = 0, 1, 2, 3, 4, 5 – each being $(2S + 1)$-degenerate. The singlet state $S = 0$ becomes the ground state for $J > 0$ (corresponding to AFM coupling), where J is the exchange constant. The relative energies of the states are 0, J, $3J$, $6J$, $10J$ and $15J$. The EPR integrated intensity $I_{int}(T)$ arising from a multiplet of total spin S can be calculated from the Boltzmann law, yielding the following expression for a pair of exchange-coupled Fe^{3+} ions:

$$I_{int}(T) = \frac{1}{T}\Big[C_1\exp(-J/kT) + C_2\exp(-3J/kT) + C_3\exp(-6J/kT) + C_4\exp(-10J/kT) + C_5\exp(-15J/kT)\Big]/Z \quad (1)$$

where $Z = 1 + 3\exp(-J/kT) + 5\exp(-3J/kT) + 7\exp(-6J/kT) + 9\exp(-10J/kT) + 11\exp(-15J/kT)$ is the partition function and the coefficients C_i (i = 1,…,5) are adjustable parameters related to the transition probability within each multiplet of total spin S. The solid line in Fig. 8(b), represents the best fit to the experimental data for the first maximum (at 40 K) with an AFM exchange constant of J = 18(1) K. This value is significantly smaller than that obtained for an isostructural $Mg_3Fe_4V_6O_{24}$ compound (J = 53(2) K) [5]. In Fig. 8(c), a similar fit is presented for the lowest temperature maximum (about 6 K). The fit is satisfactory and the value of the obtained AFM exchange constant is J = 6(2) K. Thus, two different subsystems of iron dimers exist in β-$Cu_3Fe_4V_6O_{24}$. This is consistent with the crystallographic structure of this material, in which Fe1 and Fe2 pairs can be distinguished. In Fig. 8(d), the temperature dependence of the product $T \times I_{int}$ is presented. This product is proportional to the square root of the effective magnetic moment. A decrease in $T \times I_{int}$ on cooling is an evidence of the existence of AFM interactions in the entire temperature range.

A comparison of the temperature dependence of static dc susceptibility and the EPR integrated intensity I_{int} shows large differences, especially in the low temperature range ($T < 40$ K). These differences can be explained by regarding that I_{int}, in contrast to the dc magnetization, reveals dynamic spins at the EPR spectrometer frequency (∼9.5 GHz). Thus, the spin system in β-$Cu_3Fe_4V_6O_{24}$ investigated by a static method could produce quite different results than the same system observed on a short time scale (∼10^{-10} s) of the EPR spectrometer. Short-lived spin clusters which are likely to be present in the investigated material might contribute to I_{int}, but not to the static magnetic susceptibility.

Although the exact origin of the observed EPR signal is difficult to establish, a consistent picture can be obtained, assuming that at high temperatures, the exchange-coupled Fe^{3+} spin occupying both Fe1 and Fe2 sites contributes to the EPR signal, whereas at lower temperatures ($T < 40$ K), a short-range order occurs, reducing the EPR intensity and the divergent behavior of the g-factor and the linewidth. Two low-temperature peaks observed in the magnetic susceptibilities (the dc magnetization and the EPR integrated intensity) indicate the existence of at least two separate spin populations, one stemming from the Fe1 dimers, and the other from the Fe2 dimers. It cannot be excluded that the population of Fe ions placed at

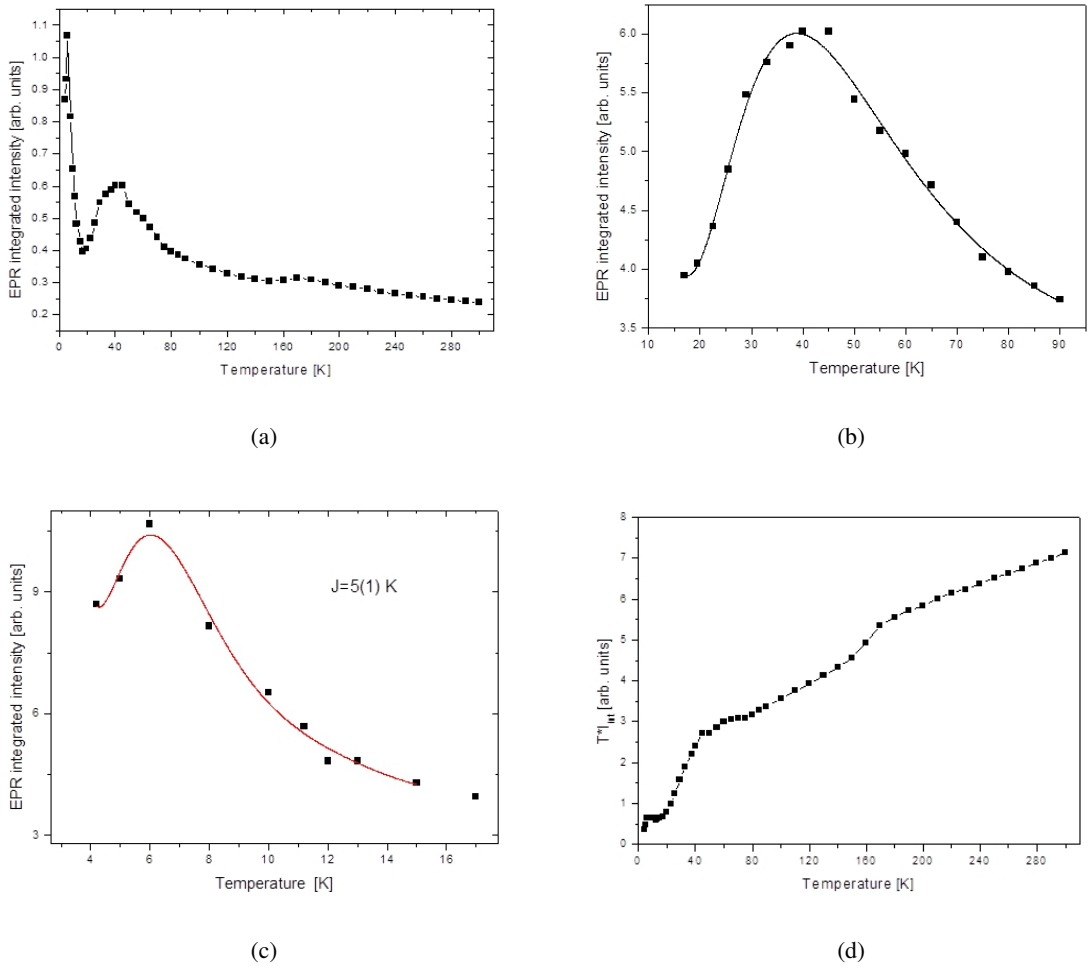

Fig. 8. Temperature dependence of a) the integrated intensity I_{int} in the entire temperature range; b) the integrated intensity in 15 – 90 K range; c) the integrated intensity in 4 – 17 K range; and d) the product $I_{int} \times T$. The solid lines in panels b and c are the best fits to the Eq. 1.

Cu sites forms yet another spin-cluster type. The differences in the transition temperatures registered from the dc magnetization and EPR measurements could be blamed on different dynamics scales revealed by a particular method of observation. The magnetic inhomogeneity of low-temperature β-$Cu_3Fe_4V_6O_{24}$ is thus the result of the occurrence of specific units in the crystal structure and is further promoted by cation site disorder. The presence of oxygen deficiency, confirmed by the presence of a small fraction of magnetic vanadium spins (e.g. V^{4+} with $S = 1/2$) can disrupt the exchange coupling of the Fe^{3+} magnetic moments.

4. Conclusions

Significant magnetic inhomogeneity has been found in the β-$Cu_3Fe_4V_6O_{24}$ compound. In the high temperature range, a strong antiferromagnetic interaction, with a Curie-Weiss temperature of $\theta \approx -80$ K, was measured. ZFC magnetization revealed the presence of two spin-glass transitions at $T_{f1} = 4.4$ K and $T_{f2} = 3.0$ K, respectively, which are related to the two types of the Fe^{3+} dimers. In EPR measurements, similar peaks were observed in the integrated intensity, however, their corresponding temperatures were shifted to 40 K and 6 K, respectively. This temperature difference can be explained by the use of different

time scales in these two methods. The magnetic inhomogeneity revealed at low temperatures in the β-$Cu_3Fe_4V_6O_{24}$ compound could result from specific crystallographic circumstances (different sublattices with cation site disorder) and oxygen deficiency.

References

[1] LAFONTAINE M. A., GRENECHE J. M, LALIGANT Y, FEREY G., *J. Solid State Chem.*, 108 (1994), 1.

[2] WANG X., VAN DER GRIEND D. A., STERN C. L., POEPPELMEIR K. P, *J. Alloy. Compd.*, 298 (2000), 119.

[3] LIKODIMOS V. et al., *Eur. Phys. J. B*, 38 (2004), 13.

[4] ZOLNIERKIEWICZ G., GUSKOS N., TYPEK J., BLONSKA-TABERO A., *J. Non-Cryst. Solids*, 352 (2006), 4362.

[5] GUSKOS N. et al., *J. Appl. Phys.*, 101 (2007), 103922.

[6] GUSKOS N. et al., *J. Non-Cryst. Solids*, 355 (2009),1419.

[7] GUSKOS N. et al., *Radiat. Eff. Defect. S.*, 158 (2003), 369.

[8] GUSKOS N. et al., *J. Alloy. Compd.*, 377 (2004), 47.

[9] GUSKOS N. et al., *J. Alloy. Compd.* 391 (2005), 20.

[10] BESKROVNYJ A., GUSKOS N., TYPEK J., RYABOVA N. YU., BLONSKA-TABERO A, KURZAWA M., ZOLNIERKIEWICZ G., *Rev. Adv. Mater. Sci.*, 12 (2006), 166.

[11] BEZKROVNYJ A. et al., *Mater. Sci.-Poland*, 23 (2005), 883.

[12] LAVES G. et al., *Phys. Rev. Lett.*, 93 (2004), 247201.

[13] LAVES G. et al.,, *Phys. Rev. Lett.*, 95 (2005), 087205.

[14] SZYMCZAK R., BARAN M., FINK-FINOWSKI J., GUTOWSKA M., SZEWCZYK A., SZYMCZAK H., *Phys. Rev. B* 73 (2006), 094425.

[15] ZOLNIERKIEWICZ G., GUSKOS N., TYPEK J., ANAGNOSTAKIS E. A., BLONSKA-TABERO A., BOSACKA M., *J. Alloy. Compd.*, 471 (2009), 28.

[16] GUSKOS N., TYPEK J., ZOLNIERKIEWICZ G., BLONSKA-TABERO A., KURZAWA M., LOS S., KEMPINSKI W., *Mater. Sci.-Poland*, 24 (2006), 985.

[17] GUSKOS N., TYPEK J., ZOLNIERKIEWICZ G., BLONSKA-TABERO A., KURZAWA M., BOSACKA M., *Mater. Sci.-Poland*, 23 (2005), 923.

[18] KURZAWA M., BLONSKA-TABERO A., *Mater. Res. Bull.*, 37 (2002), 849.

[19] LIKODIMOS V. et al., *Phys. Rev. B*, 54 (1996), 12342.

[20] ZOLNIERKIEWICZ G., TYPEK J., GUSKOS N., BOSACKA M., *Appl. Magn. Reson.*, 34 (2008), 101.

[21] NAGATA K., ISHIHARA A., *J. Magn. Magn. Mater.*, 104/7 (1992), 1571.

Received 2012-01-01
Accepted 2012-03-07